Available online at www.sciencedirect.com

SCIENCE DIRECT

Biochimica et Biophysica Acta 1669 (2005) 116–124

BIOCHIMICA ET BIOPHYSICA ACTA BBA

http://www.elsevier.com/locate/bba

Precision parameters from spin-probe studies of membranes using a partitioning technique. Application to two model membrane vesicles

Miroslav Peric*, Marilene Alves, Barney L. Bales

Department of Physics and Astronomy and The Center for Supramolecular Studies, California State University at Northridge, Northridge, CA 91330-8268, United States

Received 13 October 2004; received in revised form 13 January 2005; accepted 14 January 2005
Available online 17 March 2005

Abstract

A new version of the ESR spin probe partitioning method is developed and applied to the study of hydration properties of dimyristoyl-phosphatidylglycerol (DMPG) and dimyristoyl-phosphatidylcholine (DMPC) vesicles as functions of salt concentration and temperature above the lipid phase transition. The small spin probe di-*tert*-butyl nitroxide (DTBN) is used in order to achieve motionally narrowed Electron Spin Resonance (ESR) spectra which may be analyzed with high precision. The new method relies on the use of the second harmonic display of the ESR spectrum followed by spectral line fitting. Spectral fitting yields precise ESR parameters giving detailed information on the surroundings of the spin probe in both phospholipid and aqueous phases. The nitrogen hyperfine coupling constant of DTBN arising from those probes occupying the vesicles is used to study the hydration of the vesicle surface. The hydration properties of the negatively charged vesicle surface of DMPG vesicles are affected by the addition of salt at all temperatures. In contrast, the hydration of DMPC vesicles does not change with salt concentration at the low temperatures. However, at higher temperatures the hydration properties of DMPC vesicle are affected by salt which is interpreted to be due to the faster motion of the phospholipid molecules. The partitioning of the spin probe increases with salt concentration for both DMPG and DMPC vesicles, while water penetration decreases simultaneously. The spin probe in the phospholipid bilayer exhibits anisotropic motion and the extent of the anisotropy is increased at the higher salt concentrations.

Keywords: Electron Spin Resonance spectroscopy; Membrane hydration; Dimyristoyl-phosphatidylglycerol vesicle; Dimyristoyl-phosphatidylcholine vesicle; Spin probe; Spectral line fitting

1. Introduction

Most biological molecules, like lipids and proteins, have hydrophobic and hydrophilic parts governing their interactions with the water surrounding them, called hydration water. Both lipids and proteins are two major constituents of biological membranes, which separate cells from the extracellular environment. The lipid molecules are arranged in a continuous lipid bilayer providing the basic structure of the biological membrane and serving as a highly impermeable barrier to the passage of most ions and water-soluble molecules. Protein molecules moving freely in the lipid bilayer perform most of the specific functions of the membrane. Therefore, hydration water is not only important for the stability and flexibility of biological membranes, but also influences the structure and function of them. A number of experimental methods may be used for studying the structural and dynamical properties of hydration water, including time-resolved fluorescence quenching [1,2], deuterium nuclear magnetic resonance [3,4], neutron scattering [5], differential scanning calorimetry [6,7] and electron spin resonance (ESR) [8,9].

Recently, it has been shown that the spin probe ESR technique can be used to study the surface hydration of micelles to high precision [10,11]. In the same work a simple geometric model of the micelle, based upon a spherical hydrocarbon core with very little water penetration surrounded by a concentric polar shell, was proposed in order to describe the hydration of the polar shell. The model

* Corresponding author. Tel.: +1 818 677 2944; fax: +1 818 677 3234.
E-mail address: miroslav.peric@csun.edu (M. Peric).

0005-2736/$ - see front matter © 2005 Elsevier B.V. All rights reserved.
doi:10.1016/j.bbamem.2005.01.012

predicts the volume fraction of the polar shell occupied by water as a function of micelle size that is in excellent agreement with experiment. In micelle work, long-chain flexible spin probes have proved to be useful because spectra in the motional narrowing regime are obtained allowing high precision parameters to be extracted.

The spin probe ESR technique has extensively been used for studying model and biological membranes [12–14], because spin probes are sensitive and informative monitors of their environment [12]. The rationale to use long-chain spin probes in the study of aggregates is the fact that their hydrophobicity assures that a predominate fraction of the probes reside within the aggregates uncomplicated by an ESR signal arising from probes residing in the aqueous fraction of the sample. Unfortunately, often when these probes are used to study membranes and vesicles motionally narrowed spectra are no longer obtained. Spectra that are broadened due to slower motions can often be analyzed using computer simulation techniques pioneered by Freed [15,16]; however, the high precision is lost and, often, ambiguities enter due to the increased number of adjustable parameters that enter into the analysis.

Motionally narrowed spectra can still be obtained in a wide variety of aggregates using small spin probes; however, very often these small probes partition into the aqueous fraction producing spectra that are superpositions of the signal in the aggregate and in the aqueous phase. To simplify the language in this paper, we abbreviate the reference to these signals as the "lipid" and the "water" signals, respectively. Small nitroxides have been used for many years to study various aggregates, usually with the emphasis on the partition coefficient [17,18]. In the present technique, the partition coefficient will still be available, with high precision; however, our emphasis is on obtaining high precision ESR parameters from the lipid and the water signals. Small spherical spin probes, like DTBN (di-*tert*-butyl nitroxide) and TEMPO (4-oxo-2,2,6,6-tetramethylpiperidinyloxy) and its derivatives, have been used in studies of lipid phase transitions [19] and membrane bilayer fluidity [20]. When these small nitroxide probes partition between the fluid hydrophobic regions of the lipids membrane phase and the surrounding aqueous medium the partitioning coefficient can be measured from the ESR spectrum [19]. In most cases, at X-band only the high field lines originating from the hydrocarbon and aqueous phases are well resolved and the partition coefficient is defined in terms of their heights. The partition coefficient calculated in this manner will be in error if differences in activation energies for probe motion in the two media affect the ESR lines differently [21]. In order to improve the resolution of spin probe partitioning ESR spectra two different strategies have been employed. The first strategy is based on the use of perdeuterated nitroxides, but only perdeuterated DTBN has all three resonances from each phase well resolved at X-band [20,22]. The second strategy is to perform partitioning experiments at higher microwave frequencies [8,23] taking advantage of the enhanced *g*-value resolution. A disadvantage of higher frequencies is that the same enhanced *g*-value resolution can lead to slow motion effects that can be neglected at X-band.

Nonlinear least-square spectral fitting has become a very important tool for data analysis in ESR spectroscopy [24,25]. Due to spectral fitting and the development of modern magnetic field sweeps, which are exceptionally linear and reproducible, it is now possible to measure line positions and widths with a precision of a few mG. In addition to this extraordinary precision, spectral fitting also supplies precise line shapes and intensities.

The purpose of this work is to detail the method and demonstrate its use in the study of the hydration state of dimyristoyl-phosphatidylglycerol (DMPG) and dimyristoyl-phosphatidylcholine (DMPC) vesicles. The method detailed here utilizes X-band microwave frequencies to minimize slow-motion effects and because this is the equipment available to most labs. We employ a third strategy of resolution enhancement, using second harmonic detection, which is followed by spectral fitting.

It is well known that metal ions can change the ability of phospholipid molecules to attract water, and thus the hydration state of the membrane surface. Here we use Na^+ ions to modify the hydration of DMPG and DMPC vesicles.

2. Materials and methods

2.1. Materials

The sodium salt of the phospholipid DMPG (1,2-dimyristoyl-*sn*-glycero-3-[phospho-*rac*-(1-glycerol)], lot 140PG-1170) and the phospholipid DMPC (1,2-dimyristoyl-*sn*-glycero-3-phosphocholine, lot 140PC-169) were obtained from Avanti Polar Lipids (Birmingham, AL, USA). The spin probe DTBN (di-*tert*-butylnitroxide) was bought from Molecular Probes (Junction City, OR, USA). The buffer system used was 10 mM Hepes (4-(2-hydroxyethyl)-1-piperizineethanesulfonic acid) adjusted with NaOH to pH 7.4. PTFE tubing was a gift from Fluortek (Easton, PA, USA).

2.2. Lipid dispersion preparation

Solutions of DMPG and DMPC were made in chloroform and then dried under a stream of N_2. Thereafter, the samples were kept under reduced pressure overnight. Vesicles were prepared by the addition of buffer solution and the desired concentration of salt, followed by vortexing above the phase transition for 10 min. The samples were then sonicated with a Virsonic 50 Ultrasonicator for 15 min (30 s sonication followed by 30 s pause) at a power of 2 W. All vesicle solutions became translucent suspensions of single walled vesicles during the sonication. The appropriate amount of DTBN was added to produce a concentration of

0.2 mM spin probe solution. To insure the uniformity of the spin probe the vesicle dispersions were additional vortexed for 1 min. Finally, the samples were drawn into 15 cm long PTFE tubes of 0.5 mm i.d. and 0.08/0.13 mm wall thickness, whose ends were folded and tightened with a strip of parafilm (American National Can, Greenwich, CT).

2.3. ESR spectroscopy experiments

ESR measurements were performed with a Bruker ESP 300 E spectrometer equipped with a Bruker variable temperature unit (Model B-VT-2000). The PTFE tube with the vesicle/DTBN solution was inserted in a quartz tube of 4 mm o.d. (Wilmad Glass Co Cat No. 412) with a hole in the bottom to allow nitrogen equilibration of the sample [22]. This arrangement deoxygenates the samples [26]. The thermocouple tip was placed in the quartz tube so that when the tube was positioned inside the variable temperature dewar insert the tip was just outside of the sensitive region of the ESR cavity. The temperature was measured with an Omega temperature indicator (model DP41-TC-S2) and it was stable and repeatable within ± 0.2 °C from measurement to measurement. Samples were equilibrated at each temperature for at least 5 min.

Three second harmonic ESR spectra were acquired for each sample using a sweep time of 84 s; microwave power, 5 mW; time constant, 20.5 ms; sweep width, 50.2 G; modulation amplitude, 0.5 G. Although this amplitude of modulation is close to the linewidth of the ESR signal from the water phase it did not affect the resolution of the spectrum, nor the extraction of the Lorentzian linewidth [27]. The modulation amplitude broadened the Gaussian linewidth as expected [28]. Spectra were analyzed by a computer program, which performs nonlinear least-square fitting of the experimental ESR spectrum using a model of a Lorentzian–Gaussian function [24,29]. The Voigt line shape, which best describes the spin probe ESR lines in the fast motional region [30], is nearly perfectly approximated by the Lorentzian–Gaussian sum function that can be described by two different forms depending on the normalization. The first one is normalized to unit peak-to-peak amplitude, while the second is normalized to unit doubly integrated intensity [24]. The fitting program uses both forms and the results presented in this work are mostly the average of the values from the two fits. Fitting to the doubly integrated intensity sum equation was constrained to assume that all three lines from each phase have the same doubly-integrated intensity. The partition ratio, P, of DTBN in the lipid fraction is then computed as the ratio of the doubly-integrated lipid ESR line intensity to the total ESR line intensity.

ESR linewidths can be used to obtain information about the reorientational motion of spin probes in liquids. It is well known that in the fast-motion limit the peak-to-peak width of an individual ESR Lorentzian line is given by [13]:

$$\Delta B_{\mathrm{L}}(m) = A + Bm + Cm^2 \tag{1}$$

where m is the m-th component of the nitrogen nuclear spin, A is the Lorentzian linewidth of the central line, $\Delta B_{\mathrm{L}}(0)$, and terms B and C are:

$$B = \frac{1}{2}\Delta B_{\mathrm{L}}(0)\left\{\frac{\Delta B_{\mathrm{L}}(+1)}{\Delta B_{\mathrm{L}}(0)} - \frac{\Delta B_{\mathrm{L}}(-1)}{\Delta B_{\mathrm{L}}(0)}\right\} \tag{2a}$$

$$C = \frac{1}{2}\Delta B_{\mathrm{L}}(0)\left\{\frac{\Delta B_{\mathrm{L}}(+1)}{\Delta B_{\mathrm{L}}(0)} + \frac{\Delta B_{\mathrm{L}}(-1)}{\Delta B_{\mathrm{L}}(0)} - 2\right\}. \tag{2b}$$

Terms B and C can be used to calculate the rotational correlation times for isotropic motion according to the motional narrowing theory [13,31]. In the correlation time range τ <0.07 ns the B and C terms are simulated as a function of the relaxation times τ_{B} and τ_{C} for DTBN [13], respectively. Then the data are fitted to polynomial functions, so τ_{B} and τ_{C} can be found from B and C according to the following equations:

$$\begin{aligned}\tau_{\mathrm{B}} = {} & 0.57017B + 27.993B^2 + 208.38B^3 \\ & - 2.2789 \times 10^4 B^4 + 3.6251 \times 10^5 B^5 \\ & - 18.2159 \times 10^5 B^6 \text{ ns}\end{aligned} \tag{3a}$$

$$\begin{aligned}\tau_{\mathrm{C}} = {} & 1.7361\ C - 22.909\ C^2 + 653.01\ C^3 - 8455.3\ C^4 \\ & + 40968\ C^5 \text{ ns}.\end{aligned} \tag{3b}$$

In the range 0.07×10^{-9} s<τ<1×10^{-9} s Eqs. (3a) and (3b) take the simple forms:

$$\tau_{\mathrm{B}} = -1.415\ B \text{ ns} \tag{4a}$$

$$\tau_{\mathrm{C}} = 1.40\ C \text{ ns}. \tag{4b}$$

3. Results and discussion

Typical first harmonic and second harmonic ESR spectra of DTBN in aqueous dispersions of DMPG equilibrated with nitrogen above the phase transition are shown in Fig. 1. The second harmonic ESR spectrum shows better resolution, even though it was taken with a modulation amplitude of 0.642 G that is almost 3 times larger than the amplitude of modulation of the first harmonic spectrum, which is 0.256 G. The improved resolution of the second harmonic display is most obvious on the center field lines of DTBN. The asymmetry of the first harmonic display of the center field line is the only indication of a mixture of two lines, Fig. 1a, while the second harmonic display of the center field lines shows two separated lines, Fig. 1b.

Fig. 2a shows an experimental spectrum of DTBN in DMPG vesicles at 31.4 °C and 250 mM salt and Fig. 2b its fit to the sum of second harmonic Lorentzian and Gaussian lines. The difference between the experimental spectrum and the fit, displayed in Fig. 2c, shows a slight imperfection of the fit due to small admixture of instrumental dispersion

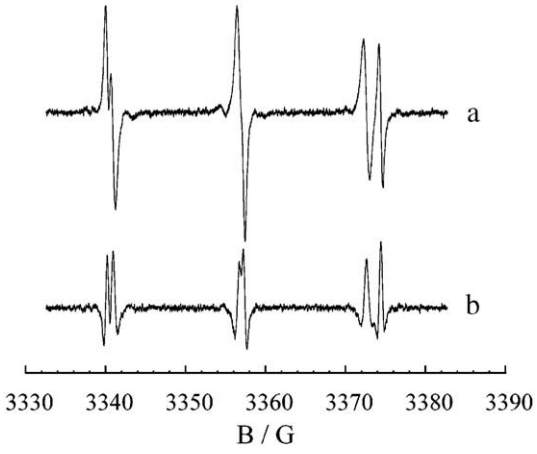

Fig. 1. ESR spectra of 0.2 mM DTBN in 100 mM DMPG vesicles in buffer equilibrated with nitrogen at 42 °C. (a) First and (b) second harmonic representations. Note the increased resolution of the second harmonic ESR spectrum.

often encountered with aqueous samples [32]. Note that this dispersion in not due to spin exchange since it is the same for all three lines. Since this dispersion is the same for all three lines it can be easily separated from spin exchange induced dispersion, which depends upon hyperfine manifold [33,34]. The dispersion may be included in the fitting procedure; however we have shown that the ESR line positions and linewidths are negligibly affected [33]. In this work, spin exchange induced dispersion is negligible due to the low DTBN concentration. The symmetry of the lipid ESR lines indicates that there is no microscopic ordering of the spin probe and the probe sampling only one region in the vesicle [21,23].

Through electrostatic and hydration interactions the polar heads of lipids in biological membranes and vesicles attract water molecules, anions and cations modulating the hydration properties of the polar shell. Fig. 3 shows the nitrogen hyperfine coupling constant of DTBN in the lipid bilayer, $A_{L,}$ of DMPG vesicles and corresponding concentration of water [H_2O] in the polar shell as a function of temperature at different salt concentrations. Note the scale of the ordinate in Fig. 3 showing that rather subtle effects of salt addition and temperature variation are easily resolved. Hydrogen bonding contributes considerably to the change in nitrogen hyperfine coupling constant when the spin probe is surrounded with water molecules [8,10,35]. Therefore, the value of A_L is a measure of the hydration state of the vesicle surface. The surface of the DMPG vesicles is negatively charged [36] and as expected increasing the concentration of salt, that is Na^+ ions, increases the hydrophobicity of the vesicle surface at all temperatures. As the sodium concentration in the aqueous phase increases, the polar heads attract more Na^+ ions decreasing the polarity of the surface, which in turn through weakened hydrogen bonding pulls less water molecules to the polar shell.

To determine the amount of water in the polar shell of the vesicle, the value of the nitrogen hyperfine spacing A_0 was measured as a function of the hydrophilicity index H defined by Mukerjee et al. [37] to be the ratio of molar concentration of OH dipoles in a solvent or solvent mixture to that in water at 25 °C. It is straightforward to show that dissolving any compound possessing N_{OH} OH bonds per molecule in water, yields the hydrophilicity index:

$$H(x,T) = \frac{\rho(x,T)M_{H_2O}}{\rho(0,25)}\left(\frac{xN_{OH}}{M} + \frac{1-x}{M_{H_2O}}\right), \quad (5)$$

where $\rho(x,T)$ is the density of the solution and x is the weight fraction of the solute of molecular weight M. The density of water at 25 °C and its molecular weight are given

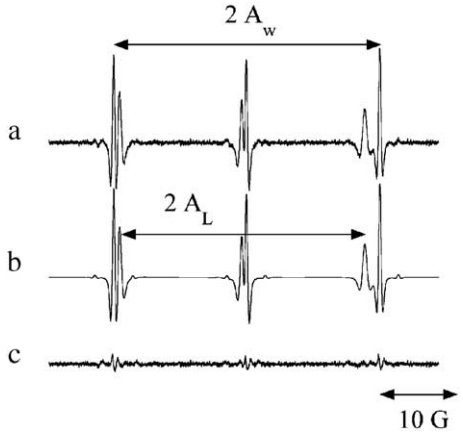

Fig. 2. (a) ESR spectrum of 0.2 mM DTBN in 100 mM DMPG vesicles with 250 mM NaCl in Hepes buffer equilibrated with nitrogen at 31.4 °C. (b) Best fit to a Voigt lineshape including the C-13 lines of the ESR signal originating from the aqueous phase. (c) Difference in the best fit and the spectrum. A_W and A_L are one half the distance between the outer lines of the ESR signal originating from the aqueous and lipid bilayer phases, respectively.

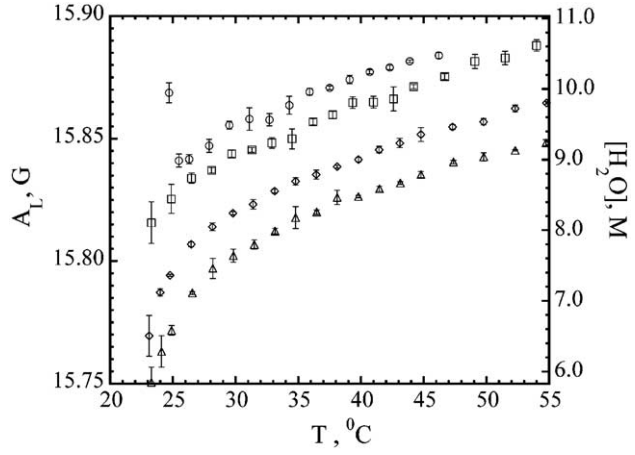

Fig. 3. Nitrogen hyperfine coupling constant A_L of 0.2 mM DTBN in the presence of 100 mM DMPG in Hepes buffer equilibrated with N_2 at pH 7.4 (left-hand ordinate) and corresponding effective water concentration [H_2O] in the polar shell calculated from Eq. (6) (right-hand ordinate) as a function of temperature. Symbols used identify the different salt concentrations and are: (○) 0 mM, (□) 125 mM, (◇) 250 mM, and (△) 500 mM. Error bars are standard deviations of three measurements.

by ρ(0,25 °C) and M_{H_2O}, respectively. If the solute does not have any OH dipoles, N_{OH}=0 and the first term in parenthesis of Eq. (5) becomes 0, or if the solvent is nonpolar, that is, without OH dipoles, then the second term in parenthesis of Eq. (5) is zero. Solutions of DTBN were prepared in a series of mixtures of ethanol–water and ethanol–dioxane. The mean values of five measurements of A_0 in each mixture are shown in Fig. 4 as a function of H(25 °C). The standard deviations are smaller than the symbols. Fitting the data to a line gives A_0=15.582+1.597H with a coefficient of correlation r=0.997. Thus the values of A_0 may be converted to values of H which, multiplied by the molar concentration of OH bonds in water at 25 °C, 55.345 M, yields the molar concentration of water which are the right-hand ordinates of Figs. 3–5. In other words, the effective water concentration in moles can be calculated from the hyperfine coupling constant A_0 using the equation:

$$[H_2O] = \left(\frac{A_0 - 15.582}{1.597}\right)55.345. \quad (6)$$

Fig. 5 shows the nitrogen hyperfine coupling constant of DTBN A_L in the polar shell of DMPC vesicles and corresponding water concentration [H_2O] as a function of temperature at different salt concentrations. Comparing Figs. 3 and 5 one can see that the effect of Na^+ on the hydration of the surface for DMPC vesicles is quite different. Just above the phase transition, around 24 °C, the addition of salt does not change the value of [H_2O] in DMPC vesicles indicating that the hydration layer is not affected by the increased salt concentration in the aqueous phase. At higher temperatures, the addition of salt starts increasing the hydrophobicity of the vesicle surface. This behavior can be explained by the structure of the phosphatidylcholine head group and the motion of the phospholipid molecules. Even though the phosphocholine polar head is neutral its negative and positive charges are separated, with the negative charge

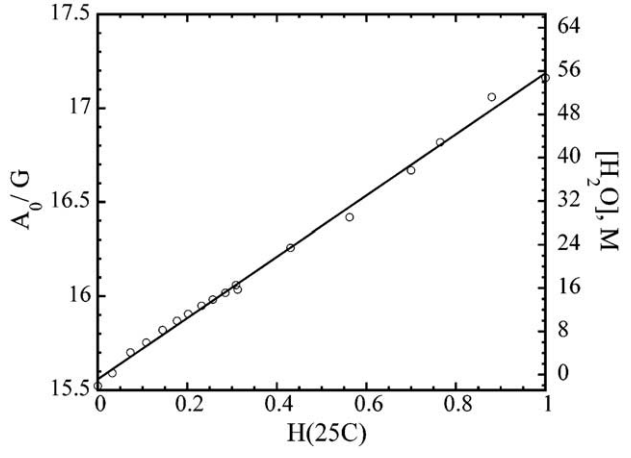

Fig. 4. Nitrogen hyperfine spacing A_0 for DTBN and effective water concentration [H_2O] calculated from Eq. (6) as a function of the hydrophilicity index H(25 °C) in a series of ethanol–water and ethanol–dioxane mixtures. The solid line is a linear least-square fit to the data. A_0=15.582+1.597H (correlation coefficient=0.997).

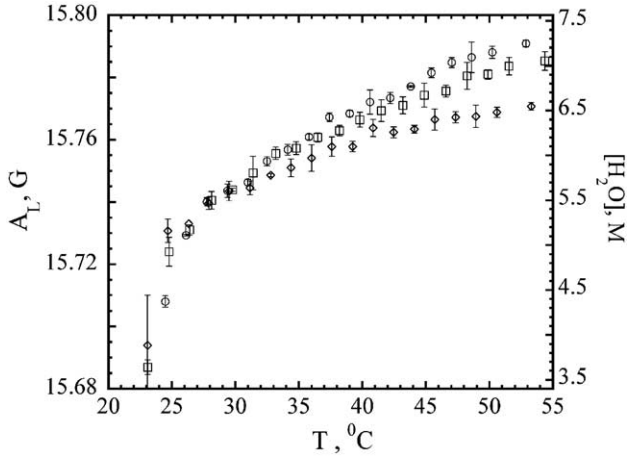

Fig. 5. Nitrogen hyperfine coupling constant A_L of 0.2 mM DTBN in the presence of 100 mM DMPC in buffer equilibrated with N_2 at pH 7.4 (left-hand ordinate) and corresponding effective water concentration [H_2O] in the polar shell calculated from Eq. (6) (right-hand ordinate) as a function of temperature. Symbols used identify the different salt concentrations and are: (○) 0 mM, (□) 250 mM and (◇) 500 mM. Error bars are standard deviations of three measurements.

localized on the phosphate group and the positive charge at the position of the nitrogen in the choline group. This tends to repel sodium ions. At lower temperatures, the phospholipid molecules are tightly packed offering a stearic and electrostatic hindrance to the entrance of sodium ions. At the higher temperatures due to thermal motions, the phospholipid molecules are less densely packed and sodium ions have slight access to the hydration layer changing the interactions of water molecules with the vesicle surface, Fig. 5.

The effect of salt on the aqueous fraction may also be studied as shown in Fig. 6 which shows the N^{14} hyperfine

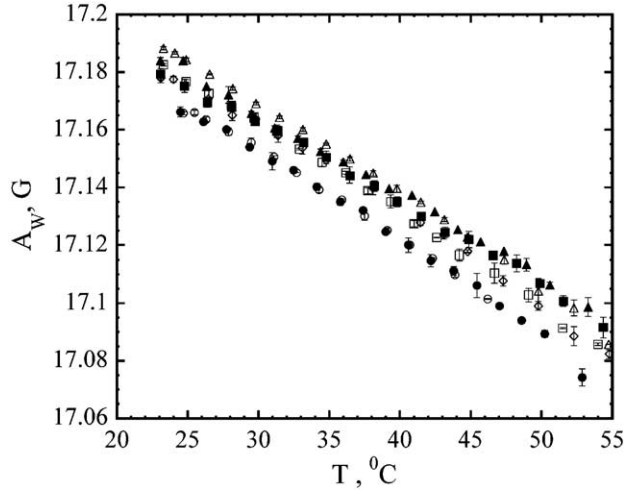

Fig. 6. Temperature dependence of A_W of 0.2 mM DTBN in the presence of 100 mM phospholipid vesicles in buffer equilibrated with N_2 at pH 7.4. The different salt concentrations and phospholipids are identified as follows: DMPG vesicles, (○) 0 mM NaCl, (□) 125 mM NaCl, (◇) 250 mM NaCl, and (△) 500 mM NaCl; DMPC vesicles, (●) 0 mM NaCl, (■) 250 mM NaCl, and (▲) 500 mM NaCl. Error bars are standard deviations of three measurements.

coupling constant of DTBN in the water A_W in DMPC and DMPG vesicles as a function of temperature at different salt concentrations. The value of A_W increases with the concentration of salt at a given temperature. Even though the change in hyperfine is very small, about 10 mG, our measurements indicate clearly that the major change is produced at a lower concentration of salt. For instance, adding 0.125 M salt to DMPG vesicles produced a bigger change in A_W than the additional increase of 0.125 M. The effect is saturated at 0.5 M NaCl (see Fig. 6). The observed increase in A_W with increasing salt concentration agrees with the fact that the affect of Na^+, which is a marginally strong polar kosmotrope (water-structure maker) [38], on water structure is slightly stronger than the effect of Cl^-, which is a weak chaotrope (water-structure breaker) [38]. The values of A_W measured in DMPG and DMPC vesicle in the absence of salt as a function of temperature overlap almost perfectly. This supports the model that DTBN in the water fraction samples predominately the volume removed from the vesicle surface unaffected by dissociated counterions in DMPG which would be expected to alter the water properties.

The hyperfine coupling constants A_W and A_L are temperature dependent. Thus it is useful to define a quantity to measure surface hydrophobicity that takes into account the changes in the density of water with temperature. Here, we define the hydrophobicity gradient $\delta A = A_W - A_L$ where A_W and A_L are the hyperfine coupling constants of DTBN in the aqueous and lipid bilayer phases, respectively. The hydrophobicity gradient also takes into account any change in the hydration of the surface produced by the change in the aqueous phase. Also, it enables the comparison of the hydrophobicity at different temperatures. Fig. 7 shows the hydrophobicity gradient of DTBN in DMPC and DMPG

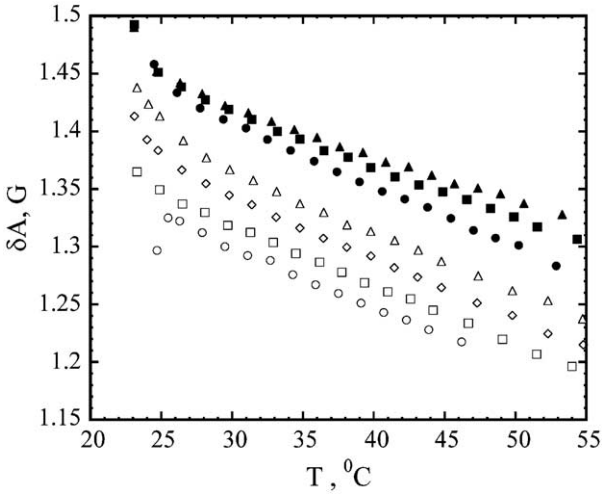

Fig. 7. Hydrophobicity gradient δA of 0.2 mM DTBN in 100 mM phospholipid vesicles in Hepes buffer at pH 7.4 as a function of temperature. The different salt concentrations and phospholipids are identified as follows: DMPG vesicles, (○) 0 mM NaCl, (□) 125 mM NaCl, (◇) 250 mM NaCl, and (△) 500 mM NaCl; DMPC vesicles, (●) 0 mM NaCl, (■) 250 mM NaCl, and (▲) 500 mM NaCl. Error bars are standard deviations of three measurements.

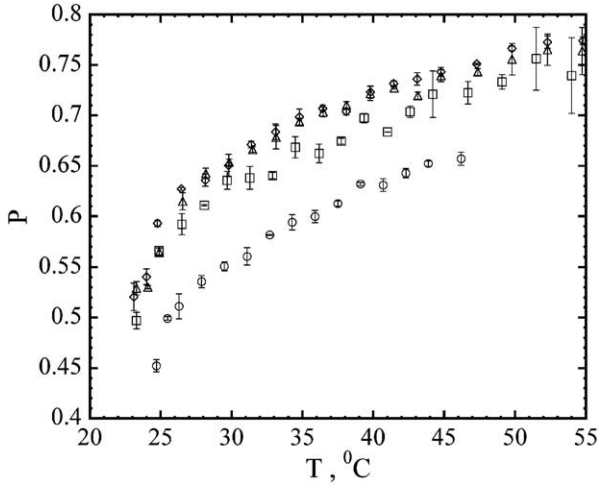

Fig. 8. Partition ratio P of 0.2 mM DTBN in 100 mM DMPG phospholipid vesicles in Hepes buffer at pH 7.4 as a function of temperature. Symbols used identify the different salt concentrations and are: (○) 0 mM NaCl, (□) 125 mM NaCl, (◇) 250 mM NaCl, and (△) 500 mM NaCl.

vesicle dispersions at different salt concentrations as a function of temperature. As is expected the surface of DMPC vesicles is more hydrophobic than the surface of DMPG vesicles. The decrease in hydrophobicity with increasing temperature can be explained by increased water binding due to an increase of area per phospholipid [3].

Fig. 8 shows the partition ratio P of DTBN in DMPG vesicles at different salt concentrations as a function of temperature. The spin probe partitioning in the lipid phase, as expected, increases with the temperature. An increase in temperature promotes the motion of the phospholipid tails expanding the area per phospholipid making more free space for water and DTBN molecules. The partitioning of DTBN also increases with the concentration of salt. As in the case of the nitrogen hyperfine coupling constant in the water A_W, Fig. 8, the addition of 0.125 M salt produced a bigger jump in partitioning than did the additional addition of the same or larger amount of salt. The partitioning of DTBN in DMPC vesicles, which is not shown, behaves in the same way as in DMPC vesicles. The increased salt concentration enhances the solubility of the spin probe in the bilayer. Finally, our data clearly indicate that the spin probe partitioning is larger in DMPG than in DMPC vesicles at a given salt concentration. This may be due to the negatively charged surface of DMPG vesicles providing more free space accessible to water and DTBN molecules in these vesicles than in DMPC vesicles under the same ionic strength conditions.

Rotational correlation times τ_B and τ_C determined from the experimental spectra of DMPC vesicles at different salt concentrations as a function of temperature by using Eqs. (3a, 3b) and (4a, 4b) are shown in Fig. 9. The results for τ_C and τ_B of DTBN in DMPG vesicles, not shown here, are very similar to the DMPC results. In the fast motional regime, for small nearly spherical spin probes rotating in isotropic liquids Eqs. (4a) and (4b) give $\tau_B = \tau_C$, and any discrepancy between the rotational correlation times τ_B and

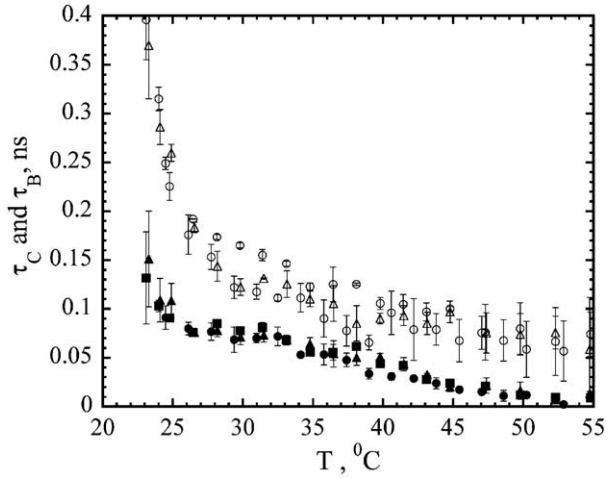

Fig. 9. Rotational correlation times τ_C and τ_B 0.2 mM DTBN in 100 mM DMPC phospholipid vesicles in Hepes buffer at pH 7.4 as a function of temperature. Symbols used identify the different salt concentrations and are: τ_C—(○) 0 mM NaCl, (□) 250 mM NaCl, and (△) 500 mM NaCl; and τ_B—(●) 0 mM NaCl, (■) 250 mM NaCl, and (▲) 500 mM NaCl. Error bars are standard deviations of three measurements.

τ_C provides information about the extent of anisotropy of the spin probe motion. At all temperatures the value of τ_C is greater than that of τ_B, which is an indication of the anisotropic rotational diffusion of the DTBN in the lipid phase. The ratio τ_C/τ_B is a measure of the anisotropy of the motion of the spin probe. Also its value indicates the preferential molecular axis of rotation [31]. The ratio τ_C/τ_B as a function of temperature has the same general features for all DMPC and DMPG vesicles. The value of τ_C/τ_B decreases slightly above the phase transition, levels out in the temperature range 25–40 °C, and then starts increasing above 40 °C. At the higher temperatures the intensity of the ESR lines decreases. The value of τ_C/τ_B for both DMPC and DMPG vesicles, averaged over the temperature range 25–40 °C, as a function of salt concentration is given in Table 1. For all concentrations the value of τ_C/τ_B is greater than 1 meaning that the preferential axis of rotation is the molecular *y*-axis, which is parallel to the line connecting the two *tert*-butyl groups. The value of τ_C/τ_B in Hepes is 1.49±0.09. Thus, the probe rotates about its longest molecular axis both in water and bilayer. The fact that the values in the bilayer are just slightly greater than in the aqueous phase suggests that the probe is probably not located deep in the hydrocarbon region, but close to the vesicle surface. Also, the data in Table 1 suggest that the anisotropy of the DTBN rotation increases with the concentration of salt.

Table 1
Values of τ_C/τ_B for both DMPC and DMPG vesicles, averaged over the temperature range 25–40 °C, as a function of salt concentration

[NaCl] mM	τ_C/τ_B—DMPC	τ_C/τ_B—DMPG
0	1.84±0.23	1.69±0.37
125		2.28±0.22
250	1.95±0.20	2.24±0.21
500	2.92±0.40	2.90±0.38

τ_C/τ_B (Hepes)=1.49±0.09.

Finally, Fig. 10 shows the nitrogen hyperfine coupling of DTNB in the bilayer of DMPC and DMPG vesicles as a function of the partition ratio of DTBN in the lipid for different salt concentrations. One can observe that A_L, in other words the amount of water in the polar shell for a given salt concentration, is a linear function of the partition ratio. This means that the partition ratio is correlated with the penetration of water molecules. The fact that all the lines have about the same slope implies that the rate of water penetration produced by increasing the temperature is the same for different salt concentrations and different phospholipids. Thus, the increase in partitioning comes only from the faster motion of the phospholipid tails, which produces more space among phospholipid molecules. In order to explain the experimental data presented above we use a slightly modified version of the four-region model of the phospholipid bilayer proposed by Marrink and Berendsen [39] based on computer simulations of DPPC. Our model, shown in Figs. 11 and 12, assumes that the first region contains bulk water and any additives to the system. The second region, the hydration layer, is the interface between phospholipids and water whose width is defined by a drop in headgroup density from 90% to 10%. In the case of negatively charged phospholipids this region contains counterions too. The density of this region is the highest in the system. The remaining two regions are the same as in the four-region model of Marrink and Berendsen. The third region is composed of partially ordered hydrocarbon tails with no water penetration. According to computer simulations this region is the main barrier to permeation of small

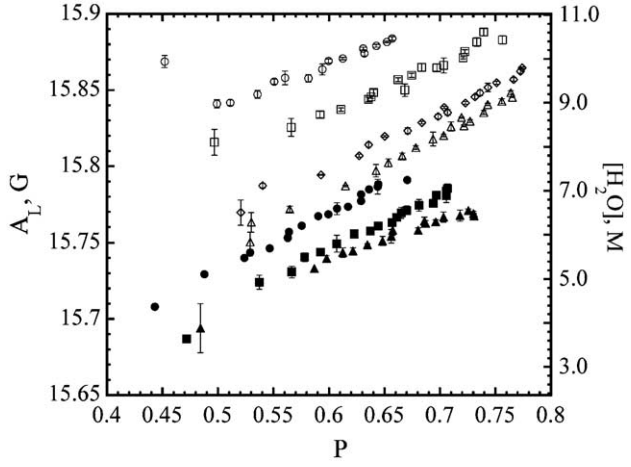

Fig. 10. Nitrogen hyperfine coupling constant A_L of 0.2 mM DTBN in the presence 100 mM phospholipid vesicles in Hepes buffer at pH 7.4 (left-hand ordinate) and corresponding effective water concentration [H_2O] in the polar shell calculated from Eq. (6) (right-hand ordinate) as a function of the partition ratio, *P*. The different salt concentrations and phospholipids are identified as follows: DMPG vesicles, (○) 0 mM NaCl, (□) 125 mM NaCl, (◇) 250 mM NaCl, and (△) 500 mM NaCl; DMPC vesicles, (●) 0 mM NaCl, (■) 250 mM NaCl, and (▲) 500 mM NaCl. Error bars are standard deviations of three measurements.

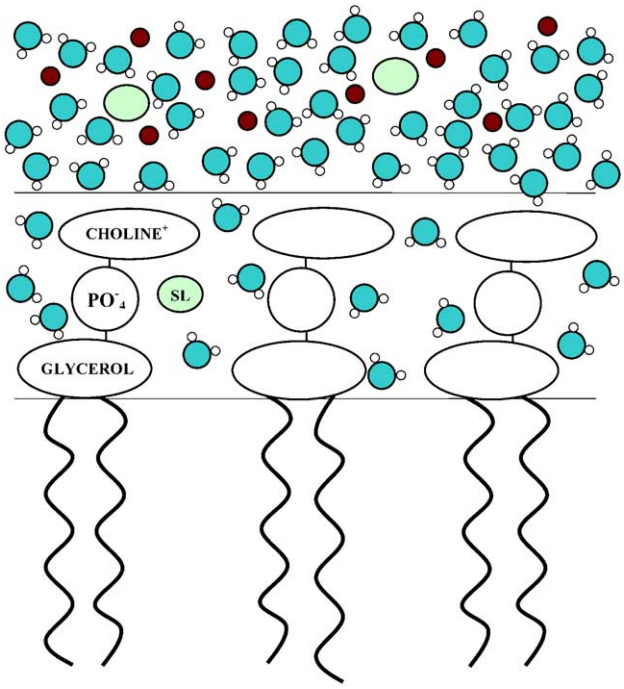

Fig. 11. Schematic of the DMPC vesicle. Three different regions are shown: the aqueous phase consisting of water molecules (a blue circle with two small circles), DTBN spin probes (SL, green ellipses) and sodium ions (brown circles); the hydration layer consisting of phospholipid headgroups (Glycerol, PO_4^- and $Choline^+$), water molecules and DTBN spin probes; and the phospholipid bilayer (hydrocarbon tails).

molecules [39]. Although the fourth region, the middle of the bilayer, has the same chemical composition as the third region, its density is much lower and resembles that of decane, and thus has distinctively different physical properties [39]. This region is not shown in Figs. 11 and 12.

Our data are consistent with the spin probe DTBN being partitioned only between the first and second regions, and that no spin probe resides in the middle of the phospholipid bilayer. Firstly, the value of A_W indicates that part of the spin probe is in the water. Secondly, the difference in the value of A_L for DMPC and DMPG vesicles as well as different behavior with salt indicates that the second signal comes from two different environments. The hydration layer is the only region in these vesicles that is different. Thus the spin probe is very likely to be in the hydration region. Also, it might be possible that some of this spin probe samples part of the phospholipid layer close to the vesicle surface. If this is the case, the effect of the third region on the ESR signal is the same for both DMPC and DMPG vesicles, and therefore A_L reports only on the hydration layer.

We propose that the decrease in A_L in DMPG vesicles with salt concentration is due to a dehydration of the hydration layer as the concentration of salt increases. Sodium ions reside in both the hydration layer and the aqueous phase. The negatively charged headgroups keep the concentration of the sodium ions in the hydration layer constant, thus if the concentration of Na^+ in the aqueous phase increases, water will move from the hydration layer to the aqueous phase. In DMPC vesicles, the addition of salt does not affect the hydration of the vesicle surface, so there is no change in hyperfine coupling constant.

4. Conclusions

We have shown that membranes may be studied with small probes leading to ESR parameters of high precision. This is the preferred approach when hydrophobic probes yield ESR spectra slower than the fast motion regime. The new version of the ESR spin probe partitioning, consisting of the second harmonic display and spectral fitting, can be very useful in studying the hydration properties of phospholipid vesicles. The use of the second harmonic detection increases the resolution of the ESR spectrum, while spectral fitting, as expected, greatly improves the precision of the ESR parameters extracted from both aqueous and lipid phases. The method ought to be rather general as long as a suitable small probe can be found that provides a usable range of partitioning. Given the vast number of probes now available, this likely will not pose a problem; however, testing of candidate probes would be a prerequisite to an investigation. The enhanced precision of the extracted ESR parameters give detailed information on the surroundings of the spin probe. The experimental results provide evidence that DMPG vesicles are more hydrated then the DMPC vesicle is, which is consistent with the literature. Also, the hydration

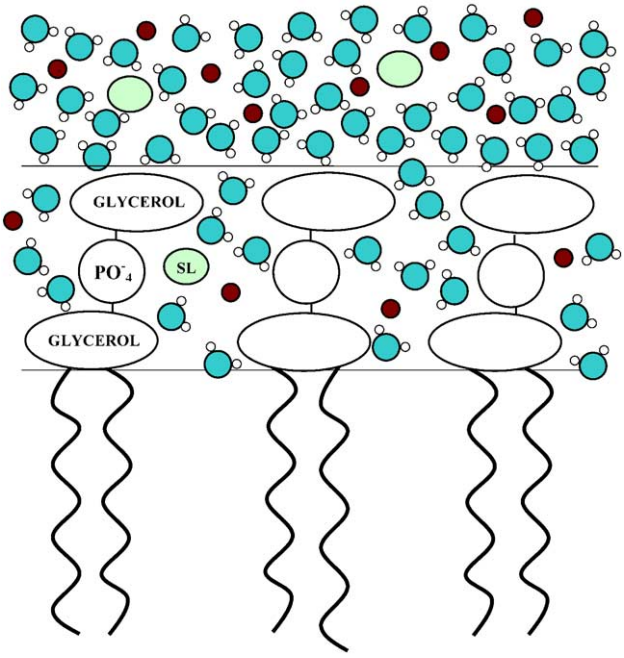

Fig. 12. Schematic of the DMPG vesicle. Three different regions are shown: the aqueous phase consisting of water molecules (a blue circle with two small circles), DTBN spin probes (SL–green ellipses) and sodium ions (brown circles); the hydration layer consisting of phospholipid headgroups (Glycerol, PO_4^- and Glycerol), water molecules, sodium ions and DTBN spin probes; and the phospholipid bilayer (hydrocarbon tails).

of the surface of DMPG vesicles decreases with the salt concentration, while the hydration state of DMPC vesicles is much less affected by the addition of NaCl. The hydration of the vesicle surface in the liquid crystal phase increases with the increase in temperature.

Acknowledgements

The authors gratefully acknowledge support from NIH Grants 5 S06 GM48680-09 (BLB) and 3 S06 GM48680-10S1 (MA and MP).

References

[1] C. Ho, S.J. Slater, C.D. Stubbs, Hydration and order in lipid bilayers, Biochemistry 34 (1995) 6188–6195.
[2] C. Ho, C.D. Stubbs, Effect on *n*-alaknols on lipid bilayer hydration, Biochemistry 36 (1997) 10630–10637.
[3] K. Arnold, L. Pratsch, K. Gawrisch, Effect of poly(ethylene Glycol) on phospholipid hydration and polarity of the external phase, Biochim. Biophys. Acta 728 (1983) 121–128.
[4] B. Bechinger, J. Seelig, Conformational changes of the phosphatidylcholine headgroup due to membrane dehydration. A ^{2}H-NMR study, Chem. Phys. Lipid 58 (1991) 1–5.
[5] J. Fitter, R.E. Lechner, N.A. Dencher, Interactions of hydration water and biological membranes studied by neutron scattering, J. Phys. Chem., B 103 (1999) 8036–8050.
[6] A.S. Ulrich, M. Sami, A. Watts, Hydration of DOPC bilayer by differential scanning calorimetry, Biochim. Biophys. Acta 1191 (1994) 225–230.
[7] D. Bach, I.R. Miller, Hydration of phospholipid bilayers in the presence and absence of cholesterol, Biochim. Biophys. Acta 1368 (1998) 216–224.
[8] O.H. Griffith, P.J. Dehlinger, S.P. Van, Shape of the hydrophobic barrier of phospholipid bilayers (evidence for water penetration in biological membranes), J. Membr. Biol. 15 (1974) 159–192.
[9] W.K. Subczynski, A. Wisnievska, J.-J. Yin, J.S. Hyde, A. Kusumi, Hydrophobic barriers of lipid bilyer membranes formed by reduction of water penetration by alkyl chain unsaturation and cholesterol, Biochemistry 33 (1994) 7670–7681.
[10] B.L. Bales, L. Messina, A. Vidal, M. Peric, O.R. Nascimento, Precision relative aggregation number determinations of SDS micelles using a spin probe. A model of micelle surface hydration, J. Phys. Chem., B 102 (1998) 10347–10358.
[11] B.L. Bales, A. Shahin, C. Lindblad, M. Almgren, Time-resolved florescence quenching and electron paramagnetic resonance studies of the hydration of lithium dodecyl sulfate micelles, J. Phys. Chem. 104 (2000) 256–263.
[12] L.J. Berliner (Ed.), Spin Labeling Theory and Applications, vol. 1, Academic Press, New York, 1976.
[13] S. Schreier, C.F. Polnaszek, I.C.P. Smith, Spin labels in membranes problems in practice, Biochim. Biophys. Acta 515 (1978) 375–436.
[14] L.R. Dalton (Ed.), EPR and Advanced EPR Study of Biological Systems, CRC Press, Boca Raton, 1984.
[15] D.J. Schneider, J.H. Freed, Calculating slow motional magnetic resonance spectra, in: J.L. Berliner, J. Reuben (Eds.), Biological Magnetic Resonance, vol. 8, Plenum, New York, 1989, pp. 1–76.
[16] D.E. Budil, S. Lee, S. Saxena, Nonlinear-least-squares analysis of slow-motion EPR spectra in one and two dimensions using modified Levenberg–Marquardt algorithm, J. Magn. Reson., Ser. A 120 (1996) 155–189.
[17] W.L. Hubbell, H.M. McConnell, Spin-label studies of the excitable membranes of nerve and muscle, Proc. Nat. Acad. Sci. U. S. A. 61 (1968) 12–26.
[18] B.L. Bales, M.E. Bauer, ESR studies of DTBN in a model lipid–water system, Chem. Phys. Lett. 7 (1970) 341–344.
[19] E.J. Shimshick, H.M. McConnell, Lateral phase separations in phospholipid membrane, Biochemistry 12 (1973) 2351–2360.
[20] F. Severcan, S. Cannistraro, Use of PDDTBN spin probe in partition studies of lipid membranes, Chem. Phys. Lett. 153 (1988) 263–267.
[21] C.F. Polnaszek, S. Schreier, K.W. Butler, I.C.P. Smith, Analysis of the factors determining the EPR spectra of spin probes that partition between aqueous and lipid phases, J. Am. Chem. Soc. 100 (1978) 8223–8232.
[22] W.Z. Plachy, D.A. Windrem, A gas-permeable ESR sample tube, J. Magn. Reson. 27 (1977) 237–239.
[23] A.I. Smirnov, T.I. Smirnova, P.D. Morse, Very high frequency electron paramagnetic resonance of 2,2,4,4-tetramethyl-1-piperidnyloxy in 1,2-dipalmitoyl-*sn*-glycero-3-phosphatidylcholine liposomes: partitioning and molecular dynamics, Biophys. J. 68 (1995) 2350–2360.
[24] H.J. Halpern, M. Peric, C. Yu, B.L. Bales, Rapid quantitation of parameters from inhomogeneously broadened EPR spectra, J. Magn. Reson., A 103 (1993) 13–22.
[25] A.I. Smirnov, R.I. Belford, Rapid quantitation from inhomogeneously broadened EPR spectra by a fast convolution algorithm, J. Magn. Reson., A 113 (1995) 65–73.
[26] J.S. Hyde, W.K. Subczynski, Spin-label oxymetry, in: L.J. Berineler, J. Reuben (Eds.), Spin Labeling: Theory and Applications, Plenum, New York, 1989, pp. 399–425.
[27] M. Peric, H.J. Halpern, Fitting of the derivative Voight ESR line under conditions of modulation broadening, J. Magn. Reson., A 109 (1994) 198–202.
[28] B.L. Bales, M. Peric, M.T. Lamy-Freund, Contributions to the Gaussian line broadening of the proxyl spin probe EPR spectrum due to magnetic-field modulation and unresolved proton hyperfine structure, J. Magn. Reson. 132 (1998) 279–286.
[29] B.L. Bales, Inhomogeneously broadened spin-label spectra, in: J.L. Berliner, J. Reuben (Eds.), Biological Magnetic Resonance, vol. 8, Plenum, New York, 1989, pp. 77–130.
[30] B.L. Bales, Correction for inhomogeneous line broadening in spin labels: II, J. Magn. Reson. 48 (1982) 418–430.
[31] S.A. Goldman, G.V. Bruno, C.F. Polnaszek, J.H. Freed, An ESR study of anisotropic rotational reorientation and slow tumbling in liquid and frozen media, J. Chem. Phys. 56 (1972) 716–735.
[32] P. Ludowise, G.R. Eaton, S.S. Eaton, A convenient monitor of EPR automatic frequency control function, J. Magn. Reson. 93 (1991) 410–412.
[33] B.L. Bales, M. Peric, EPR line shifts and line shape changes due to spin exchange of nitroxide free radicals in liquids, J. Phys. Chem., B 101 (1997) 8707–8716.
[34] M. Peric, B.L. Bales, Lineshapes of spin exchange broadened EPR spectra, J. Magn. Reson. 169 (2004) 27–29.
[35] B.L. Bales, C. Stenland, The spin probe-sensed polarity of sodium dodecyl sulfate micelles is proportional to the one-fourth power of the surfactant concentration, Chem. Phys. Lett. 200 (1992) 475.
[36] K.A. Riske, O.R. Nascimento, M. Peric, B.L. Bales, M.T. Lamy-Freund, Probing DMPG vesicle surface with a cationic aqueous soluble spin label, Biochim. Biophys. Acta 1418 (1999) 133–146.
[37] P. Mukerjee, C. Ramachandran, R.A. Pyter, Solvent effects on the visible spectra of nitroxides and relation to nitrogen hyperfine splitting constants. Nonempirical polarity for aprotic and hydroxilic solvents, J. Phys. Chem. 86 (1982) 3189–3197.
[38] K.D. Collins, Sticky ions in biological systems, Proc. Nat. Acad. Sci. U. S. A. 92 (1995) 5553–5557.
[39] D.P. Tieleman, S.J. Marrink, H.J.C. Berendsen, A computer perspective of membranes: molecular dynamics studies of lipid bilayer systems, Biochem. Biophys. Acta 1331 (1997) 235–270.